Label-free imaging of thick tissue at 1550nm using a femtosecond optical parametric generator

Johanna Trägårdh,[1,*] Gillian Robb,[1] Kamal K.E. Gadalla,[2,3] Stuart Cobb,[2] Christopher Travis,[4] Gian-Luca Oppo,[4] and Gail McConnell,[1]

[1]*Centre for Biophotonics, SIPBS, University of Strathclyde, 161 Cathedral Street, Glasgow, G4 0RE, UK*
[2]*Institute of Neuroscience and Psychology College of Medical, Veterinary and Life Sciences University of Glasgow,West Medical Building,Glasgow G12 8QQ, UK*
[3]*Pharmacology Department, Faculty of Medicine, Tanta University, Egypt*
[4]*Department of Physics, University of Strathclyde, 107 Rottenrow, Glasgow, G4 0NG, UK*

**Corresponding author: johanna.tragardh@strath.ac.uk*

Received Month X, XXXX; revised Month X, XXXX; accepted Month X, XXXX; posted Month X, XXXX (Doc. ID XXXXX); published Month X, XXXX

We have developed a simple wavelength tunable optical parametric generator (OPG), emitting broad band ultrashort pulses with peak wavelengths at 1530-1790 nm, for nonlinear label-free microscopy. The OPG consists of a periodically poled lithium niobate crystal, pumped at 1064 nm by a ultrafast Yb:fiber laser with high pulse energy. We demonstrate that this OPG can be used for label-free imaging, by third harmonic generation, of nuclei of brain cells and blood vessels in a >150 μm thick brain tissue section, with very little decay of intensity with imaging depth and no visible damage to the tissue at an incident average power of 15 mW .

OCIS Codes: (180.4315) Nonlinear microscopy, (190.2620) Harmonic generation and mixing, (190.4970) Parametric oscillators and amplifiers.

Label-free imaging allows for the study of biological samples without chemical modifications and the associated sample preparation that could modify the structure or mechanism under study. In label-free third harmonic generation (THG) imaging, the image contrast arises from refractive index differences within the specimen, as well as from differences in 3rd order susceptibility $\chi^{(3)}$ [1], with the THG signal being generated across the interfaces [2]. This allows for label-free visualization of, for example, blood vessels and red blood cells [3,4], lipid structures [1,5], cell boundaries and membranes [5,6] and brain tissue [3,7-9]. Since THG imaging is a nonlinear imaging method, it provides inherent optical sectioning as well as larger imaging depth than simpler label-free imaging methods such as differential interference contrast (DIC). Furthermore, for imaging deep into brain tissue, it has been shown that three-photon imaging has potential for retaining the resolution and therefore support imaging deeper into thick grey matter than two-photon imaging [7,10]. Since no optical energy is deposited in the tissue, in contrast to in fluorescence imaging, the sample damage is potentially low, despite the high laser peak powers needed. However, the use of THG in biological imaging has been limited by the available laser sources. As THG is a third order nonlinear process, ultra-short laser pulses are required to generate sufficiently high peak powers for efficient signal generation. Furthermore, these pulses should preferably be at longer wavelengths than those available with a Ti:Sapphire laser (>1080nm) because the detected wavelength, which is a third of the excitation wavelength, is otherwise in the UV wavelength range, where standard microscope optics, as well as the tissue itself, have low transparency. Longer excitation wavelengths also give larger penetration depth in tissue because of reduced scattering [7], as well as less specimen damage [11].

The laser should also be tunable so that the wavelength can be chosen to suit the scattering properties of the sample. The tunable fs-pulsed lasers available at these longer wavelengths, in particular for reaching the tissue transparency window at 1300nm and beyond, are Cr:Forsterite lasers at 1220-1270nm [6], commercially available optical parametric oscillators (OPOs) and homebuilt OPOs [11]. The former are costly, and the latter are challenging to build and to maintain, in particular in a bio-imaging facility where laser expertise may not be available. Fiber lasers have also been used for THG imaging, although at their intrinsic fixed wavelengths [12,13]. Fiber lasers have also been used as pump lasers for tunable systems employed for THG imaging, based on pumping a nonlinear optical fiber [14] where the tuning was achieved by adjusting the pre-chirp of the pulse and, perhaps more easily implemented, using soliton self-frequency shift in a large mode area photonic crystal fiber [8] or a photonic crystal rod [7], where the generated solitons were broad band and the wavelength region could be selected with a band pass filter [7,8].

Femtosecond optical parametric generators (OPGs) emitting at suitable wavelengths for THG imaging have been discussed in the literature [15-19], including systems with 1 MHz repetition rate and μJ pulse energy [19], similar to what is demonstrated here, but have, to our knowledge, not been used for imaging or microscopy. There is an advantage to using excitation sources with lower repetition rate in the single MHz region and high peak power, since this gives more efficient THG while

keeping the average power low. Compared to a possibly more efficient optical parametric amplifier (OPA), an OPG has the advantage that no seed pulse is needed. The tunability of an OPA is limited by the seed pulse and it adds the complication of synchronous seeding for fs seed pulses [15].

In this letter we present a simple, tunable, single-pass, femtosecond OPG, pumped by a commercially available high pulse energy Yb:fiber laser. The OPG emits around 300 fs pulses and is wavelength tunable from 1530 to 1790 nm. The system is easy to setup and maintain for routine use in a bioimaging facility, and is substantially less costly than a commercial OPO. We demonstrate the use of the system by THG imaging of thick fixed brain tissue.

The OPG consisted of a 3mm-long periodically poled lithium niobate (PPLN) crystal (Covesion MOPO1-0.5-3) with period lengths of 27.9-31.6 μm, pumped at 1064 nm by a high pulse energy (1 μJ) ultrafast fiber laser (Fianium HE1060-1uJ-fs) emitting 400 fs pulses. The pump light was focused into the PPLN crystal using a f=+125 mm focal length plano-convex singlet lens (Fig. 1(a)), and the emission was collimated using a f=+25 mm focal length lens. The crystal temperature was controlled using an oven (Covesion PV10).

The output spectrum for the OPG, using 1.1 W of pump power at 1 MHz and a crystal temperature of 120 °C, is presented in figure 1(b). For these parameters 130 mW of light at wavelengths λ>1150 nm and 140 mW at λ<1000 nm was generated. The parametric generation was efficient (12% conversion efficiency to 1550 nm) because of the high pulse energy of the pump laser. There was also light generated at shorter wavelengths than shown in fig 1(b), including the third harmonic of the pump laser at 355 nm. The output power at λ>1150 nm was sufficient to use the source for nonlinear microscopy, also taking into account the lower transmission of the microscope optics (measured to 15%) at these long wavelengths compared to visible wavelengths. The emission at shorter wavelengths could potentially be used for excitation of single photon fluorescence as well as efficient short wavelength excitation of two-photon fluorescence [20] from the specimen, and the residual pump light at 1064nm could also potentially be used for two-photon excitation, though we did not explore this here.

The OPG was tunable from 1530 nm to 1790 nm by using the multiple regions with different poling periodicity of the PPLN crystal simply by translating the crystal in the beam (fig 1(c)). The pulses had a measured bandwidth of 120-255 nm (measured using an APE Wavescan, extended IR, spectrometer) and a pulse width of 240-370 fs (measured using a home-built autocorrelator based on 2-photon absorption in a Si photodiode and assuming a Gaussian pulse shape). The spectrum could be fine-tuned over a few tens of nanometres by adjusting the temperature of the PPLN crystal over the range 100 °C-180 °C.

The spectrum of the NIR emission, as well as the output power was highly stable. Time series of spectra on time scales from tens of milliseconds to 1 hour showed a standard deviation (SD) in the peak wavelength of <=1.3nm, and throughout the $1/e^2$ width of the spectrum the SD of the signal intensity at any one wavelength was <1.2 %. The SD in the total output power was 0.3% over 10 ms and 0.6% over 10 s.

For the imaging experiments, the OPG emission was filtered by a 1150 nm long pass (LP) filter (Thorlabs FEL1150) and coupled into a home built scanning multi-photon microscope. The microscope has been previously described in [11,20]. The light was focused using a Nikon Plan Fl 40X NA1.3 oil immersion objective. The generated THG signal was collected in transmission by the condenser lens (NA 0.8), filtered using a 525/39 nm band pass filter (Semrock, Brightline), and detected using a photomultiplier tube (Thorlabs PMM02). Since the THG efficiency hardly varies over the bandwidth of the pulse [21], the useable bandwidth was only limited by the detection filter. The image had 500x500 pixels with a pixel dwell time of 20 μs and we used a frame average of 4. For comparison, THG images were also obtained using a commercial OPO at a wavelength of 1550 nm, a pulse duration of 200 fs, a bandwidth of 25 nm and a repetition frequency of 80 MHz (Coherent Chameleon OPOVis). The OPG was used at a peak wavelength of 1550 nm (PPLN period 2, 130 °C) to facilitate comparison between the images acquired using the OPG and the OPO. The point spread function (PSF) was characterized by THG imaging of 1 μm latex beads dispersed in Vectashield (Vectorlabs). The axial (lateral) FWHM of the PSF was 4.9 μm (1.1 μm) for the OPG and 2.8 μm (1.0 μm) for the OPO. The larger axial PSF for the OPG was likely due to the non-Gaussian beam profile.

The mouse brain tissue sections used for imaging were prepared as follows: a mouse was transcardially perfused with 4% paraformaldehyde in 0.1 M Phosphate buffer solution (PBS). The brain was dissected out and post-fixed in the same fixation buffer for 4 hours, and then transferred into 30% sucrose in 0.1 M PBS (w/v) for 24 hours. One hemisphere was embedded in 3% agar and sectioned parasagitally using a vibratome. The sections were washed 3 times (10 minutes each) with 0.3 M PBS and mounted between a microscope slide and a Type 1.5 coverslip with hard-set Vectashield (n=1.46).

Figure 2 shows a THG image of an unlabeled section of the neocortex of a mouse brain at a depth of 50 μm, using a time-averaged power of 15 mW at the specimen plane. The cell nuclei are clearly visible as are blood vessels (indicated by an arrow). We demonstrate the inherent optical sectioning capability by acquiring images with a separation of 3.5 μm over a total depth of 155 μm (Media 1). As visible from the bottom images in the stack, we were imaging close to an edge of the slice. The imaging depth was not limited by the decay of the signal with increasing depth, but by the working distance of the objective. We note that the signal did not vary considerably throughout the depth, indicating that the decay of the signal with depth is slow enough also at this wavelength to allow deep tissue imaging. The top two images in the stack were brighter due to the strong THG signal generated at the interface between the tissue and the cover slip.

The low repetition rate and high pulse energy of the excitation allowed efficient THG at moderate excitation powers at the specimen plane (ca 15 mW) compared to the

few hundred mWs usually reported for imaging using Ti:Sapphire pumped 80 MHz repetition rate lasers [1,3,5,9]. We confirmed this by imaging the same sample using an 80 MHz repetition rate OPO. The signal was negligible when using the OPO at the same time-averaged excitation power as used when imaging using the OPG (fig 3). 1 MHz is still a sufficiently high repetition rate to allow imaging without excessive pixel dwell times.

We observed very little change in sample morphology over 30 minutes of continuous imaging at a depth of 50 μm with the OPG using a time-averaged power of 15 mW at the specimen plane, which suggests that this method did not cause significant photodamage. We confirmed that the method did not cause photodamage also to a living specimen mounted in water, by imaging a *Petunia* sp leaf mounted in water (fig 4). After 18 min of continuous THG imaging, we still observed cytoplasmic streaming in bright field, indicating specimen vitality. This is in line with the findings in [11] that heating due to water absorption at around 1500 nm does not pose a problem for imaging live specimens.

We confirmed that the contrast in the image was from a third order process by acquiring a series of images at different excitation powers. The slope of a linear fit to the log-log plot of the signal averaged over 10 cell nuclei versus excitation power was 3.5 (fig 5), confirming the THG process. There is possibly saturation of the signal at the highest excitation power.

As a comparison, a confocal single-photon image of an 800 μm thick brain slice from the same region of the brain, but stained with DAPI before mounting in Vectashield, was acquired. The image confirmed the structure of the tissue and that the THG took place at the nuclei (inset in fig. 2), since the objects in the THG image appear a similar lateral size to the nuclei in the fluorescence image. The larger apparent thickness of the nuclei in the THG image compared to the single photon image (data not shown) was due to the large height of the PSF at 1550 nm. An objective lens designed for use at 1550 nm would have improved the size of the PSF, and potentially allowed us to reduce the excitation power even further. Furthermore, since THG is a volume effect [2], objects of a similar size to the PSF, here nuclei and blood vessels, give a high signal, whereas smaller objects, that do have a boundary with a refractive index contrast, (axons and cells with quite small nuclei) will only give a very weak signal. Fixing the tissue has likely reduced the contrast between the cytoplasm and the exterior of the cell, leaving refractive index contrast primarily at the cell nucleus.

The much smaller imaging depth (the signal dropped rapidly over a few tens of μm) in one-photon fluorescence was due to a combination of scattering of the short excitation wavelength and the penetration of DAPI into the tissue. The uncertainty of the distribution of the stain highlights the usefulness of a label-free imaging method.

In conclusion, we have demonstrated label-free THG imaging deep in brain tissue using a simple excitation source in the form of a single-pass femtosecond OPG, which was wavelength tunable from 1530 to 1790 nm. The high pulse energy allowed for use of low time-averaged excitation powers and allowed imaging without inducing photo-damage.

Acknowledgement

This research was supported in part by the MRC grant MR/K015583/1 and the EPSRC grant EP/I006826/1. We also thank the Fraunhofer Centre for Applied Photonics for access to the APE Wavescan spectrometer.

References

1. D. Debarre, W. Supatto, A. M. Pena, A. Fabre, T. Tordjmann, L. Combettes, M. C. Schanne-Klein, and E. Beaurepaire, Nat. Methods **3**, 47 (2006)
2. R. Carriles, D. N. Schafer, K. E. Sheetz, J. J. Field, R. Cisek, V. Barzda, A. W. Sylvester, and J. A. Squier, Rev. Sci. Instrum., **80**, 081101 (2009)
3. S. Witte, A. Negrean, J. C. Lodder, C. P. J. de Kock, G. T. Silva, H.D. Mansvelder, and M.L. Groot, PNAS **108**, 5970 (2011)
4. S. Dietzel, J. Pircher, A. K. Nekolla, M. Gull, A. W. Brändli, U. Pohl, and M. Rehberg, PLoS ONE **9** e99615 (2014)
5. N. Olivier, M. A. Luengo-Oroz, L. Duloquin, E. Faure, T. Savy, I. Veilleux, X. Solinas, D. Débarre, P. Bourgine, A. Santos, N. Peyriéras, and E. Beaurepaire, Science **329**, 967 (2010)
6. C. K. Sun, S. W. Chu, S. Y. Chen, T. H. Tsai, T. M. Liu, C. Y. Lin, and H. J. Tsai, J. Struct. Biol. **147**, 19 (2004)
7. N. G. Horton, K. Wang, D. Kobat, C. G. Clark, F. W. Wise, C. B. Schaffer, and C. Xu, Nat. Photonics **7**, 205 (2013).
8. K.. Wang and C. Xu, Appl. Phys. Lett. **99,** 071112 (2011)
9. M. J. Farrar, F. W. Wise, J. R. Fetcho, and C. B. Schaffer, Biophys. J. **100**, 1362 (2011)
10. X. Deng, and M. Gu, Appl. Opt. **16**, 3321 (2003).
11. G. Norris, R. Amor, J. Dempster, W. B. Amos, and G. McConnell, J. Microsc. **246**, 266 (2012)
12. A. C. Millard, P. W. Wiseman, D. N. Fittinghoff, K. R. Wilson, J. A. Squier, and M. Müller, Appl. Opt. **38**, 7393 (1999)
13. K. Kieu, S. Mehravar, R. Gowda, R. A. Norwood, and N. Peyghambarian, Biomedical Optics Express **4**, 2187 (2013)
14. F. Tauser, F. Adler, and A. Leitenstorfer, Opt. Lett. **29**, 516 (2004)
15. H. Linnenbank and S. Linden, Opt. Express **22**,18072 (2014)
16. Y. Pu, J. Wu, M. Tsang, and D. Psaltis, Appl. Phys. Lett. **91**, 131120 (2007)
17. T. Südmeyer, J. Aus der Au, R. Paschotta, U. Keller, P. G. R. Smith, G. W. Ross and D. C. Hanna, J. Phys. D: Appl. Phys. **34**, 2433 (2001)
18. S.V. Marchese, E. Innerhofer, R. Paschotta, S. Kurimura, K. Kitamura, G. Arisholm, and U. Keller, Appl. Phys. B **81**, 1049 (2005)
19. C. Manzoni, R. Osellame, M. Marangoni, M. Schultze, U. Morgner, and G. Cerullo, Opt. Lett. **34**, 620 (2009)
20. J. Trägårdh, G. Robb, R. Amor, W. B. Amos, J. Dempster, and G. McConnell, J. Microsc., doi:10.1111/jmi.12255 (posted 06 May 2015, in press).
21. D. Débarre, and E. Beaurepaire, Biophys J. **15**, 603 (2007)

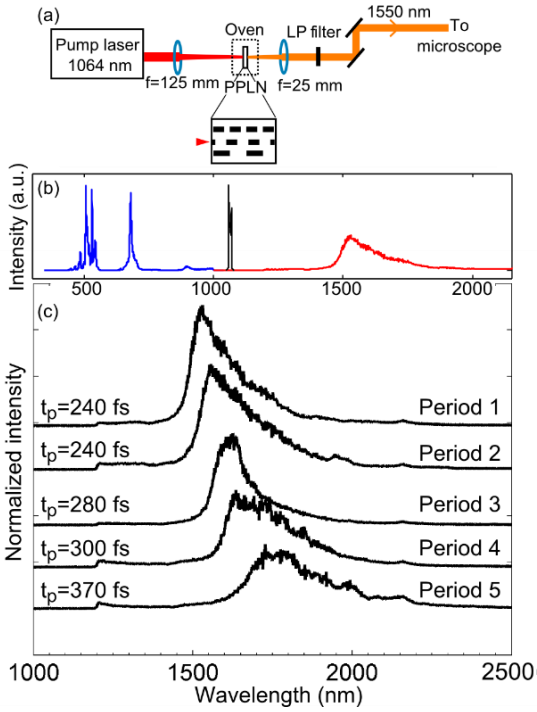

Fig 1: (a) Experimental setup showing the fs-pulsed pump laser, focused into a PPLN crystal. The output from the OPG was collimated and filtered using a LP filter before coupling into the laser scanning microscope (b) Output spectrum from the OPG using period 1 of the PPLN crystal at a temperature of 120 °C. The spectra of the pump laser and the visible and near infrared emission are not to scale. (c) Emission spectra and pulse widths t_p for the different poling periods in the PPLN crystal. The spectra are vertically offset for clarity.

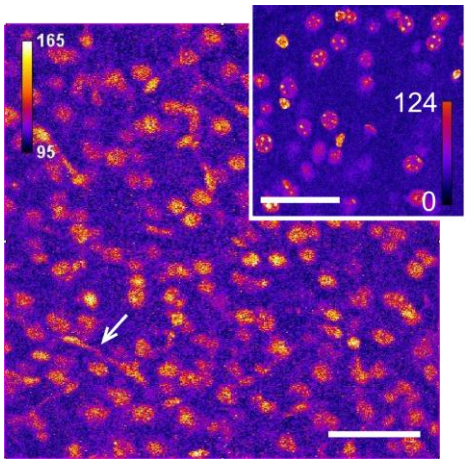

Fig 2: THG image of a parasagittal mouse brain tissue section from the neocortex, taken at a depth of 50 µm. The image shows the cell nuclei and blood vessels (one of the blood vessels is indicated by an arrow). Scale bar is 50 µm. Images were acquired with a separation of 3.5 µm over a total depth of 155 µm (Media 1). The inset shows a confocal single photon image of a section from a similar area of the brain as that imaged for figure 2, at 20 µm depth of an 800 µm thick slice stained with DAPI. Scale bar is 50 µm. The excitation was a laser diode emitting at 405 nm and the fluorescence signal was detected in the range of 420-480 nm.

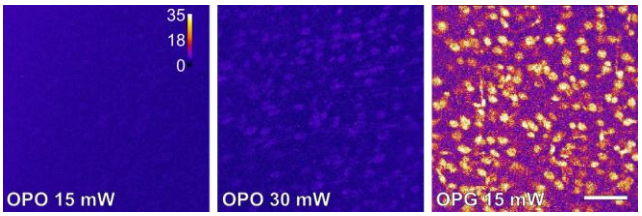

Fig 3: Comparison between excitation with an OPO at 80 MHz and 1550 nm and with the OPG. The OPG image is from a different area of the same brain slice at a comparable depth. Scale bar is 50 µm. All images are displayed with the same look-up table. The time-averaged laser power required to obtain the same signal level using the OPO was substantially higher, and for 75 mW time-averaged excitation power (the highest we used), the signal was still only 25% of that with excitation with the OPG.

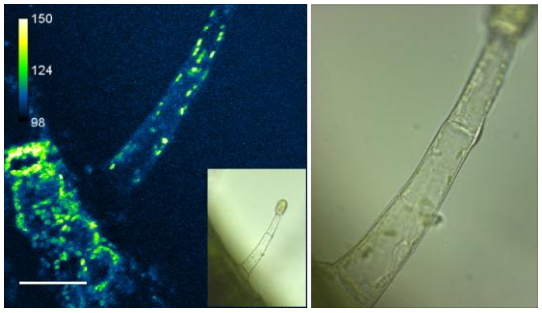

Fig 4: (a) A THG image of a hair of a *Petunia* sp leaf. Inset shows a low magnification bright field image. Scale bar is 50 µm. (b) Bright field image taken after 18 minutes of continuous imaging showing no structural damage.

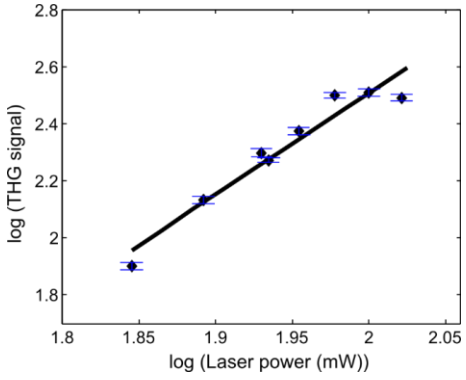

Fig 5: Excitation power dependence of the THG signal for the brain slice. Diamonds are data and the solid line is a linear fit. The slope of the linear fit is 3.5. The error bars are the standard deviation in the THG signal from 10 cell nuclei.

The full reference list

1. Debarre,D., Supatto,W., Pena,A.M., Fabre, A., Tordjmann,T., Combettes, L., Schanne-Klein, M.C. & Beaurepaire, E. "Imaging lipid bodies in cells and tissues using third-harmonic generation microscopy." Nat. Methods **3**, 47–53, (2006)
2. Carriles R., Schafer D.N., Sheetz K.E., Field J.J., Cisek R., Barzda V., Sylvester A.W., Squier J.A., "Invited review article: Imaging techniques for harmonic and multiphoton absorption fluorescence microscopy"., Rev Sci Instrum., **80**, 081101 (2009)
3. S. Witte, A. Negrean, J. C. Lodder, C. P. J. de Kock, G. T. Silva, H.D. Mansvelder, and M.L. Groot, "Label-free live brain imaging and targeted patching with third-harmonic generation microscopy", PNAS **108**, 5970–5975, 2011
4. Dietzel S, Pircher J, Nekolla AK, Gull M, Brändli AW, Pohl U., and Rehberg M.., "Label-Free Determination of Hemodynamic Parameters in the Microcirculaton with Third Harmonic Generation Microscopy." PLoS ONE **9**(6): e99615 (2014)
5. N. Olivier, M. A. Luengo-Oroz, L. Duloquin, E. Faure, T. Savy, I. Veilleux, X. Solinas, D. Débarre, P. Bourgine, A. Santos, N. Peyriéras E. Beaurepaire, "Cell Lineage Reconstruction of Early Zebrafish Embryos Using Label-Free Nonlinear Microscopy" Science **329** 967-971 (2010)
6. Sun, C.K., Chu, S.W., Chen, S.Y., Tsai, T.H., Liu, T.M., Lin, C.Y. and Tsai, H.J. "Higher harmonic generation microscopy for developmental biology." J. Struct. Biol. **147**, 19–30, 2004
7. N. G. Horton, K. Wang, D. Kobat, C. G. Clark, F. W. Wise, C. B. Schaffer, and C. Xu, "In vivo three-photon microscopy of subcortical structures within an intact mouse brain.," Nat. Photonics, **7**, 205–209, (2013).
8. K., Wang, and C. Xu, "Tunable High-Energy Soliton Pulse Generation from a Large-Mode-Area Fiber and Its Application to Third Harmonic Generation Microscopy", Applied Physics Letters **99** 071112 , (2011)
9. M. J. Farrar, F. W. Wise, J. R. Fetcho, C. B. Schaffer, "In Vivo Imaging of Myelin in the Vertebrate Central Nervous System Using Third Harmonic Generation Microscopy", Biophysical Journal, **100**, 1362–1371, (2011)
10. X. Deng, and M. Gu, "Penetration depth of single-, two-, and three-photon fluorescence microscopic imaging through human cortex structures: Monte Carlo simulation", Appl. Opt. **16** 3321-3329, (2003)
11. G. Norris, R. Amor, J. Dempster, W. B. Amos, and G. McConnell, "A promising new wavelength region for three-photon fluorescence microscopy of live cells," J. Microsc., **246**, 266–273, (2012).
12. A. C. Millard, P. W. Wiseman, D. N. Fittinghoff, K. R. Wilson, J. A. Squier, and M. Müller, "Third-harmonic generation microscopy by use of a compact, femtosecond fiber laser source", Applied Optics, **38**, pp. 7393-7397 (1999)
13. K. Kieu, S. Mehravar, R. Gowda, R. A. Norwood, and N. Peyghambarian, "Label-free multi-photon imaging using a compact femtosecond fiber laser mode-locked by carbon nanotube saturable absorber", Biomedical Optics Express, **4**, 2187-2195 (2013)
14. F. Tauser, F. Adler, and A. Leitenstorfer, "Widely tunable sub-30-fs pulses from a compact erbium-doped fiber source", Optics Letters, **29**, 516-518 (2004)
15. H. Linnenbank and S. Linden, "High repetition rate femtosecond double pass optical parametric generator with more than 2 W tunable output in the NIR", Optics Express, **22**, 18072-18077, (2014)
16. Y. Pu, J. Wu, M. Tsang, and D. Psaltis, "Optical parametric generation in periodically poled KTiOPO4 via extended phase matching", Appl. Phys. Lett. **91**, 131120, (2007)
17. T. Südmeyer, J. Aus der Au, R. Paschotta, U Keller, P. G. R. Smith, G. W. Ross and D. C. Hanna, "Novel ultrafast parametric systems: high repetition rate single-pass OPG and fibre-feedback OPO", J. Phys. D: Appl. Phys. **34**, 2433–2439 (2001)
18. S.V. Marchese, E. Innerhofer, R. Paschotta, S. Kurimura, K. Kitamura, G. Arisholm, and, U. Keller, "Room temperature femtosecond optical parametric generation in MgO-doped stoichiometric LiTaO3", Appl. Phys. B **81**, 1049–1052 (2005)
19. C. Manzoni, R. Osellame, M. Marangoni, M. Schultze, U. Morgner, and G. Cerullo, "High-repetition-rate two-color pump–probe system directly pumped by a femtosecond ytterbium oscillator", Opt. Lett. **34**, 620-622 (2009)
20. J. Trägårdh, G. Robb, R. Amor, W. B. Amos, J. Dempster, and G. McConnell, "Exploration of the two-photon excitation spectrum of fluorescent dyes at wavelengths below the range of the Ti:Sapphire laser," J. Microsc., DOI: 10.1111/jmi.12255 (posted 06 May 2015, in press).
21. D. Débarre, E. Beaurepaire, "Quantitative Characterization of Biological Liquids for Third-Harmonic Generation Microscopy", Biophys J. 15, 603-612 (2007).